Journal of the European Ceramic Society **19** (1999) 1563–1567

PII: S0955-2219(98)00478-6
0955-2219/99/$ - see front matter

Optical and Structural Characterization of Zinc Vapour Diffused Waveguides in $LiNbO_3$ Crystals

V. A. Fedorov,[a]* Yu. N. Korkishko,[a] G. Lifante[b] and F. Cussó[b]

[a]Department of Chemistry, Moscow Institute of Electronic Technology (Technical University), 103498, Moscow, Zelenograd, Russia
[b]Departamento de Física de Materiales, C-IV, Universidad Autonoma de Madrid, 28049-Madrid, Spain

Abstract

All stages of vapour Zn-diffused waveguide fabrication on different cuts of lithium niobate crystals have been structurally characterised by single- and double-crystal X-ray diffractometry. Immediately after diffusion the zinc niobate phase $ZnNb_2O_6$ was formed on the sample surface. After annealing the ZnO phase appeared with the $ZnNb_2O_6$ on the surface of the Zn-diffused waveguides. Both these phases completely disappeared after light polishing. The lattice deformations in vapour Zn-diffused waveguides were found to differ from Zn-substituted solid solutions of lithium niobate. Dark mode measurements have been used to determine the refractive-index profiles of the planar waveguides. Changes in refractive index higher than 0·05 have been obtained. © *1999 Elsevier Science Limited. All rights reserved*

Keywords: niobates, diffusion, X-ray methods, crystal structure.

1 Introduction

Lithium niobate ($LiNbO_3$) crystals have been widely used in photonics because of their excellent ferroelectric, piezoelectric, electrooptic, and nonlinear optical properties. Optical waveguides in $LiNbO_3$ have been intensively studied for applications including integrated and nonlinear optics, telecommunication systems and fiber sensors.[1] Several methods are now widely used for fabricating low-loss waveguides in this material,[1] the most popular being proton exchange and titanium in-diffusion. However, neither method produces waveguides with ideal performance for all applications. Ti-diffused waveguides guide both polarizations but suffer strong optical damage in the visible region. On the other hand, PE waveguides are much more resistant to photorefractive damage but guide only the extraordinary polarization.

Recently the possibility of fabrication of optical waveguide in $LiNbO_3$ has been demonstrated by Zn-diffusion from the vapour phase.[2,3] The planar waveguides support propagation of both TE and TM-modes, and the relationships between refractive index increase and diffusion parameters have been established.[2,3] Moreover, divalent zinc is the second (besides magnesium) damage-resistant impurity in $LiNbO_3$. It was reported that the damage resistance of $LiNbO_3$ is increased by a factor 10^2 when the crystals are heavily doped with Zn.[4] Furthermore, Zn:$LiNbO_3$ crystal did not suffer any darkening under intensive laser radiation, in contrast to Mg:$LiNbO_3$.[4] Doping with Zn has been also attempted to improve the nonlinear optical properties. Therefore Zn-diffusion in $LiNbO_3$ from a vapour phase is a new prospective technique for fabricating waveguides which can guide both polarizations and exhibit high resistance to photorefractive damage.

However, much remains unknown about the structural and optical properties of the Zn-diffused layer. The knowledge of structural phase behaviour of Zn-diffused material is quite important for the development of highly efficient waveguides, as it has been demonstrated for proton exchanged $LiNbO_3$ and $LiTaO_3$ waveguides.[1,5–8]

The aim of the present study is to identify and characterise structurally, by using single- and double-crystal X-ray diffraction techniques, all phases appearing on the different stages of optical waveguide fabrication by Zn-diffusion from the vapour phase. Dark mode technique is used to characterise the refractive-index profiles of planar vapour

*To whom correspondence should be addressed. Fax: +7-095-530-22-33; e-mail: fedorov@chem.miee.ru

Zn-diffused waveguides. From these measurements, the dependence of the ordinary (n_o) and extraordinary (n_e) refractive index changes on diffusion time and diffusion temperature has been inferred.

2 Preparation of Samples and Their Characterisation

Samples with basic X, Y and Z-cuts, as well as specially rotated Y- [(02·10), (018) and (0$\bar{1}$4)] cuts were prepared from optical grade congruent $LiNbO_3$ crystals, and then polished up to optical quality.

Zn diffusion from vapour phase has been performed using the set-up proposed and described in Ref. 2. One of the advantages of the system used to perform the diffusion is that the temperature and the Zn pressure can be controlled independently, in contrast to the conventional method of the sealed ampoule. The diffusion process was the same for all the samples studied, and was performed at a temperature of 700°C and a buffer pressure of 10 Torr for 4 h. The samples had peak values for a Zn concentration at the surface of ~4·7% and diffusion depths of ~3·0 μm.[2]

Structural phase characterisation of the zinc-diffused structures formed on different $LiNbO_3$ cuts was performed by the X-ray diffraction method. The phases were identified by using X-ray diffraction patterns obtained on all samples using Rigaku. Denki D-2 diffractometer with Ni-filtered Cu K_α radiation. Pure silicon powder was used as an internal standard. Calculation of the lattice parameters was carried out using a least-square method.

The deformations in diffused waveguiding structures were examined by analysing the rocking curves recorded by a double-crystal diffractometer DRON-3 (Si (333) monochromator, Cu $K_{\alpha 1}$ radiation) according to the method proposed.[9]

3 Results and Interpretation

A study of the ternary system of lithium, niobium and zinc oxides was undertaken by Nalbandyan *et al.*[10] and subsolidus phase equilibria in the Li_2O–Nb_2O_5–ZnO pseudo-ternary system were studied by X-ray diffraction method. The regions of solid solutions based on $LiZnNbO_4$ and most of the binary oxides were found. No solid solutions based on zinc niobate are observed in the $LiNbO_3$–$ZnNb_2O_6$ cross section.

The growth and some properties of Zn-substituted $LiNbO_3$ solid solutions sintered by the usual solid-state reaction technique at 1100°C were investigated by Kawakami *et al.*[11] A nonstoichiometric phase was identified with the formula $(Li_{1-x}Zn_{x/2})NbO_3$ (at $0 < x < 0{\cdot}25$) and a $LiNbO_3$ structure. The continuous change in the lattice parameters indicated the formation of cation vacancies produced by the substitution of a Zn^{2+} ion for two Li^+ ions in the $LiNbO_3$ lattice. Cation vacancies in these solid solutions occur at the Li-site, and the defect structure was still stable at high temperatures.[11] The solid solubility of Zn ions in $LiNbO_3$ was half that in $LiTaO_3$, which takes place at $x = 0{\cdot}5$.[12]

Figure 1 shows the diffractograms after the initial stage of Zn-diffused waveguide fabrication, that is immediately after diffusion from the Zn-vapour. They correspond to the surface plane (parallel to the surface) of zinc-diffused structures formed on basic X-, Y- and Z-cuts of $LiNbO_3$. The first characteristic that can be identified from these diffractograms and from similar recorded from inclined planes is the appearance, besides the $LiNbO_3$ peaks, of the characteristic peaks corresponding to the zinc niobate ($ZnNb_2O_6$) phase. Similar features are obtained on (02·10), (018) and (0$\bar{1}$4) rotated cuts. No peaks corresponding to $LiZnNbO_4$ (as reported by Young *et al.*[13] in waveguides fabricated in $LiNbO_3$ substrates by diffusion of a ZnO film) and $LiNb_3O_8$ were observed. These results clearly show the formation of the zinc niobate phase at the surface of the diffused sample at this stage.

The structure of $ZnNb_2O_6$ belongs to orthorhombic system (space group *Pnca*) and has the crystal lattice parameters: $a = 5{\cdot}026$ Å, $b = 14{\cdot}183$ Å and $c = 5{\cdot}727$ Å.[14,15] An inspection of the diffractograms, in Fig. 1 and of reflections from the inclined planes shows that there are the following epitaxial relationships between orientation of the substrate and that of grown zinc niobate layer: $(006)_{LN} \| (060)_{ZN}$, $(110)_{LN} \| (200)_{ZN}$, $(030)_{LN} \| (004)_{ZN}$ (Fig. 2). For the structures on the rotated cuts, the additional reflection from the surface plane exists only for (0$\bar{3}$·12) plane ((0$\bar{1}$4)-cut): $(0\bar{3}{\cdot}12)_{LN} \| (\bar{3}\ 12\ 2)_{ZN}$.

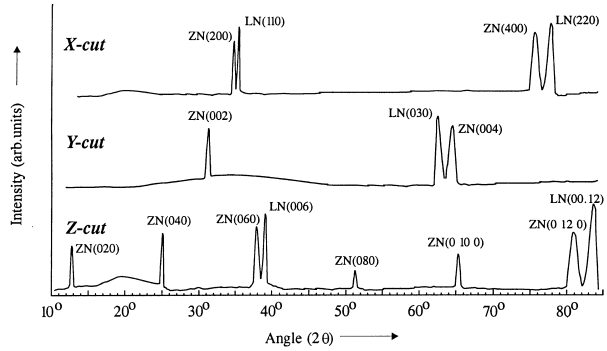

Fig. 1. Diffractograms of zinc-diffused structures formed on basic X-, Y- and Z-cuts of $LiNbO_3$ immediately after diffusion, (LN, $LiNbO_3$; ZN, $ZnNb_2O_6$).

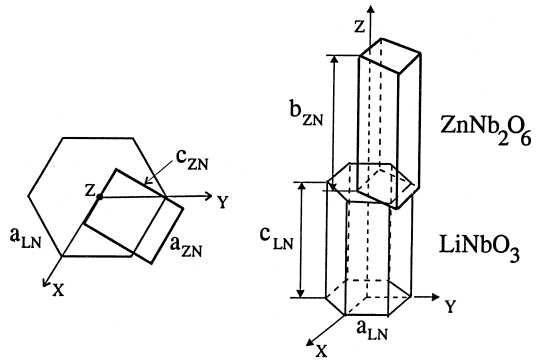

Fig. 2. Orientation of the topotaxially grown zinc niobate layer.

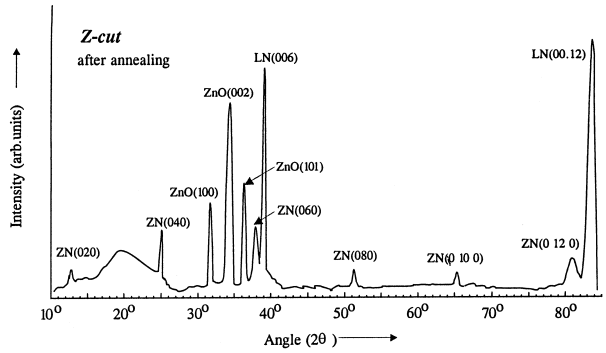

Fig. 3. Diffractogram of annealed zinc-diffused waveguide on Z-cut $LiNbO_3$.

In general, including the rotated cuts:

$$h_{ZN} = h_{LN} + k_{LN},$$
$$k_{ZN} = l_{LN}, \quad l_{ZN} = (h_{LN} - k_{LN})\cdot 2/3,$$

where $(hkl)_{LN}$ and $(hkl)_{ZN}$ are the Miller indices of parallel (equivalent) planes in the substrate $LiNbO_3$ (LN) and grown $ZnNb_2O_6$ (ZN) layer, respectively.

The next step needed for waveguide fabrication is to perform a sample annealing in open atmosphere (standard annealing conditions: 650°C, 4 h) in order to recover the transparency of the optical waveguides.[2] After this annealing, the X-ray diffractograms exhibited additional peaks corresponding to the formation of ZnO phase on the surface of Zn-diffused structures, which can be seen in Fig. 3. The peaks of $ZnNb_2O_6$ phase were still present (with reduced peak intensities after annealing) (Fig. 3).

The formation of this relatively low refractive index layer of ZnO hinders the observation of dark modes by using the standard prism coupling technique at this fabrication step. In order to be able to couple light into the waveguide, it is necessary to remove this layer by light polishing.

After the polishing, the above mentioned phases completely disappear, and the X-ray diffraction patterns are all very similar to that of pure $LiNbO_3$, except for a small broadening of the peaks, which are completely indexed on the basis of hexagonal unit cell. This corresponds to the formation of zinc-containing solid solutions with $LiNbO_3$-like structure.

In the present study the strained state in annealed and polished vapour Zn-diffused $LiNbO_3$ structures was examined according to the method described previously[9] by analysing the double-crystal X-ray rocking curves recorded in symmetric reflection for surface plane and in two asymmetric reflections from different inclined planes for each cut investigated. From the experimental diffractometric data it was calculated that Zn:$LiNbO_3$ waveguides on X- and Z-cuts have only one non-zero component ε''_{33} of the deformation tensor in the technological coordinate system appropriate to the substrate (with the axis 3″ normal to the surface plane of the plate, and 1″ and 2″ orthogonal axes lying in this plane). On Y- and rotated (02·10), (014) and (018) cuts it is found that there are two non-zero strain components ε''_{33} and ε''_{23} in this coordinate system. Therefore, it can be concluded that the zinc-diffused layers are coherent, that is, having zero in-plane deformations ε''_{11}, ε''_{12} and ε''_{22}.

To calculate the lattice parameters for unstrained Zn:$LiNbO_3$ solid solutions we have performed the experiments and calculations similar to those reported for describing the $H_xLi_{1-x}TaO_3$ and $Zn_{x/2}Li_{1-x}TaO_3$ solid solutions.[5,6] The method is based on the analysis of the strained state in the structures on the Y-rotated $(0k_sl_s)$ cuts [(02·10), (018) and $(0\bar{1}4)$ in our case] using the obtained relationships[5,6] between deformations ε''_{33} and ε''_{23}, and stress-free deformations S_a and S_c of crystal lattice cell, where $S_a = (a_L - a)/a$, $S_c = (c_L - c)/c$ and a_L, c_L and a, c are the unstrained (stress-free) lattice parameters of surface layer and substrate, respectively.

It has been found that the corresponding values for the lattice parameters range from $a = 3-4{\cdot}5 \times 10^{-4}$ and $S_c = 1{\cdot}7 - 2{\cdot}5 \times 10^{-4}$, depending on the cuts. The relationship observed between the stress free deformation parameters $S_c/S_a \approx 0{\cdot}55$ in Zn-vapour diffused layers is substantially lower than that found in Zn-substituted solid solutions, prepared and described by Kawakami *et al.*[11] where $S_c/S_a \approx 0{\cdot}93$. The value of S_c/S_a characterises the relative tension ($S_c/S_a > 1$) or compression (< 1) of the lattice cell along c axis as well as the predominant deformation in the basal (oxygen) plane (along a axes, $S_c/S_a < 1$) or perpendicular to this plane (along c axis, > 1). Although the origin of this difference is still unknown, it could be related to a different location of the zinc ions in the $LiNbO_3$ lattice in Zn vapour

diffused and Zn-substituted solid solutions, as it has been found in nonstoichiometric solid solutions of Zn in $LiTaO_3$ crystals,[6] where different phases with different S_c/S_a values have been reported.

We may therefore conclude that waveguide formation by the Zn diffusion from vapour phase is due to the formation of a lithium niobate-like structure with Zn incorporated predominantly in or near a basal (oxygen) plane. The diffused layers are characterised by low stress values and also by S_c/S_a value lower than Zn-substituted solid solutions, which suggests an interstitial location for the diffused Zn ions.

Optical characterization of the waveguides was performed by a prism coupling technique for both TE- and TM-polarized light from a He-Ne laser ($\lambda = 633$ nm). From the measured mode angles the corresponding effective indices were calculated. An inverse WKB analysis of the calculated effective indices was used to calculate an index profile for the planar waveguides. Measurements have shown in all cases the formation of planar waveguides in both ordinary and extraordinary refractive indices, the increase of n_e being slightly greater than that of n_o, in accordance with previous results[3] ($\Delta n_e = 2{\cdot}3\%$ and $\Delta n_o = 1{\cdot}9\%$ for Zn-diffused waveguides on X-cut $LiNbO_3$). These increases are at least twice as large as those obtained for Ti indiffused $LiNbO_3$, and are an order of magnitude higher than the changes in refractive indices reported for Zn-diffused $LiNbO_3$ from a ZnO source. From optical measurements the dependences of the n_e and n_o refractive index changes on diffusion time, diffusion temperature, and buffer pressure were obtained.[3] This has been possible because of the flexibility of the system used for the Zn diffusion from the vapor phase, which allows independent control of temperature, time and pressure. Both Δn_e and Δn_o increase with increasing temperature. Nevertheless, even at the lowest fabrication temperature tested (550°C), the waveguide shows a rather high index increase for $n_e(\Delta n_e = 1{\cdot}8\%)$.[3] The dependence of the waveguide depth on diffusion temperature was also plotted.[3] The calculated activation energy for vapor Zn diffusion in $LiNbO_3$ ($E_a = 1{\cdot}4$ eV[3]) is close to that found for Zn diffusion at higher temperatures from Zn oxide. It is important to note that although the diffusion coefficient is small at low temperature [D (550°C) = $0{\cdot}02\,\mu m^2\,h^{-1}$ (Ref. 3)], the change in refractive index is still high, indicating the possibility of fabricating monomode waveguides at low temperatures m convenient periods of time (~1 h).

As has been shown, the increase of n_e is slightly higher than that of n_o, regardless of diffusion time. Figure 4 depicts Δn_e versus Δn_o for X- and Z-cut samples studied.[3] As can be seen in that figure the

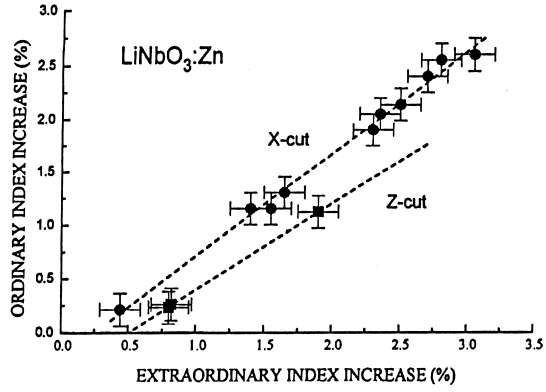

Fig. 4. Relationship between Δn_e and Δn_o for X- and Z-cut of $LiNbO_3$ waveguides fabricated by Zn vapor diffusion.

relationship between Δn_e and Δn_o shows a linear behaviour for values of $\Delta n_e > 0{\cdot}5\%$ with a slope of ~0·9.

The waveguide losses were measured for the diffused samples by use of the standard end coupling technique. Taking into account the transmission of the objective lenses, losses due to Fresnel reflections at the interfaces, and coupling mismatch losses, a value of $1{\cdot}2\,db\,cm^{-1}$ for TE and $1{\cdot}0\,db\,cm^{-1}$ for TM both at 633 nm, were obtained for 1·5 cm long-*X*-cut sample, with light polarized along the *Y* direction.[3]

Acknowledgements

The present work was supported by INTAS under project 'Active integrated optical waveguides and devices', by the Russian Foundation of Basic Researches under grant nos. 96-15-96978 and 99-15-96110 for Young Doctors of Sciences and grant no. 96-15-98220 for Leading Science Schools and by the 'Russian Universities—Basic Researches' program under grant no. 248-1998. This investigation is also part of the project K-0513 'Perspective techniques of micro- and nanoelectronics' supported by the 'Integration' Foundation (Russia).

References

1. Korkishko, Yu. N. and Fedorov, V. A., *Ion Exchange in Single Crystals for Integrated Optics and Optoelectronics*. Cambridge International Science, Cambridge UK, 1998, 506p.
2. Herreros, B. and Lifante, G., *Appl. Phys. Lett.*, 1995, **66**, 1449.
3. Schiller, F., Herreros, B. and Lifante, G., *J. Opt. Soc. Am. A*, 1997, **14**, 425.
4. Volk, T., Rubinina, N. and Pryalkin, V., *Opt. Lett.*, 1990, **15**, 996.
5. Fedorov, V. A. and Korkishko, Yu. N., *Ferroelectrics*, 1994, **160**, 185.
6. Fedorov, V. A. and Korkishko, Yu. N., *Ferroelectrics*, 1995, **166**, 181.

7. Korkishko, Yu. N. and Fedorov, V. A., *IEEE J. Selected Topics Quantum Electron.*, 1996, **2**, 187.
8. Korkishko, Yu. N. and Fedorov, V. A., *J. Appl. Phys.*, 1997, **82**, 1010.
9. Fedorov, V. A., Ganshin, V. A. and Korkishko, Yu. A., *Physica Status Solidi (a)*, 1993, **135**, 493.
10. Nalbandyan, V. B., Medvedev, B. S., Nalbandyan, V. A. and Chinenova, A. V., *Inorganic Materials*, 1988, **24**, 830.
11. Kawakami, S., Ishii, E., Tsuzuki, A., Sekiya, T. and Torii, Y., *Mat. Res. Bull.*, 1986, **21**, 463.
12. Torii, Y., Sekiya, T., Yamamoto, T., Kobayashi, K. and Abe, Y., *Mat. Res. Bull.*, 1983, **18**, 1569.
13. Young, W. M., Fejer, M. M., Digonnet, M. J. F., Marshall, A. F. and Feigelson, R. S., *J. Lightwave Technol.*, 1992, **10**, 1238.
14. Brusset, H., Mahe, R. and Aung Kyi, U., *Mat. Res. Bull.*, 1972, **7**, 1061.
15. Harrison, R. W. and Delgrosso, E. J., *J. Electrochem. Soc.*, 1963, **110**, 205.